

LIL FRONT END
DESCRIPTION AND EXPERIMENTAL RESULTS

P. Brunet, R. Chaput
Laboratoire de l'Accélérateur Linéaire
Université Paris-Sud - 91405 ORSAY Cedex France

Summary

Early in the LEP study, it was clear that we needed a good linac front-end in order to get a safety margin on the positron flux taking into account the uncertainty on the injection/ejection efficiency figures of the 5 successive machines. As neither existing experimental data nor computation program were entirely exhaustive and reliable, it was decided to specify and order, the linac front-end, a few years ahead of the rest of the machine and to test it at LAL, Orsay, taking advantage of the existing facilities.

We are presenting :

- 1 - A description of :
 - . The front-end, designed and manufactured by the C.G.R. MeV company :
 - a triode gun : 100 kV, 20 A, 12 ns ;
 - an S-band buncher : 30 MeV, standing wave, tri-periodic structure.
 - . The instrumentation developed by LAL in order to measure the beam parameters : intensity, energy, emittance, bunch length.

2 - The main results of the experimental program which took place in 1982 and 1983.

1 - Description

The installation lay-out is shown on fig.1. The 3 main parts are :

- The RF 25 MW power source and the RF power network.
- The front-end itself : gun, pre-buncher, buncher equipped with focusing coils (Ref. 1).
- The beam lines and instrumentation.

1.1 Front-end

1.1.1 Electron gun : It is a triode gun with a spherical cathode ($R = 40$ mm) of 35 mm in diameter and a grid of 2.5×2.5 mesh.

The current measured at the anode output increases linearly with the H.V. from 5 A at 40 kV to 20 A at 100 kV.

The pulse length may be adjusted from 5 to 30 nanos with rise and fall time of ~ 3 ns.

The anode output is immersed in a 0.2 T magnetic field ; the cathode is shielded by the magnetic anode plate and a counter coil.

A beam intensity monitor (cylindrical electrode) is located right after the gun anode.

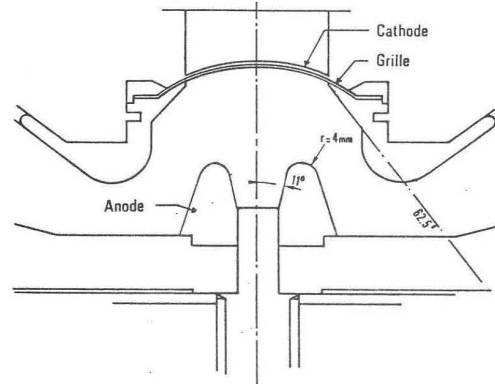


Fig. 2. Gun sketch.

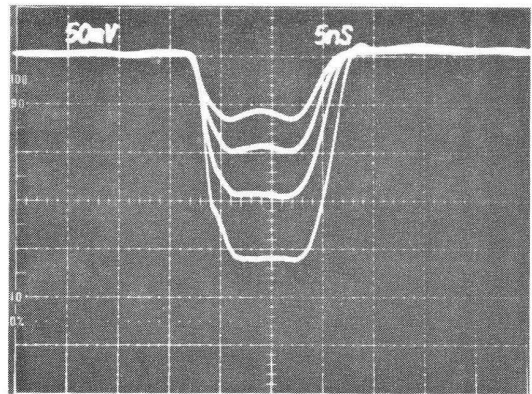


Fig. 3. Typical gun current pulse shape VS. grid voltage.

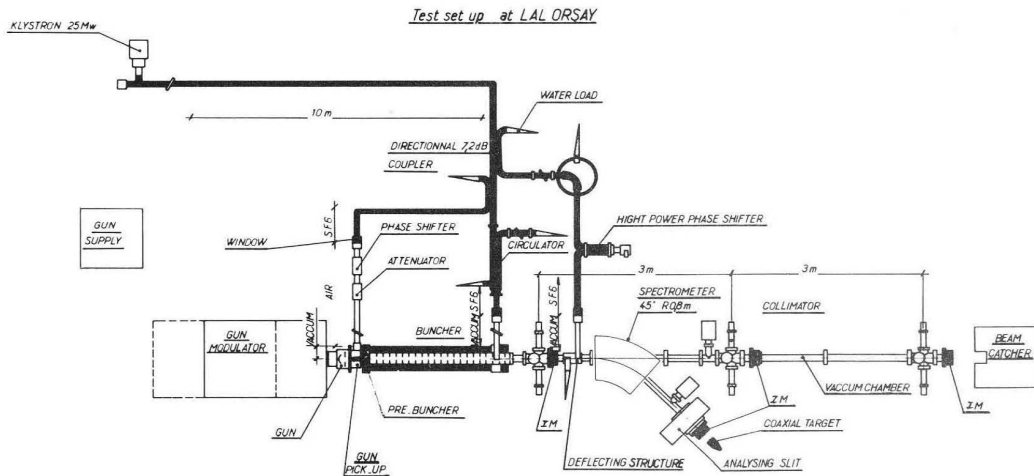


Fig. 1. Test set up of the LIL Front End.

1.1.2 . Buncher : It is a 2.2 meters, S-band ($\lambda = 10$ cm), triperiodic standing wave structure :

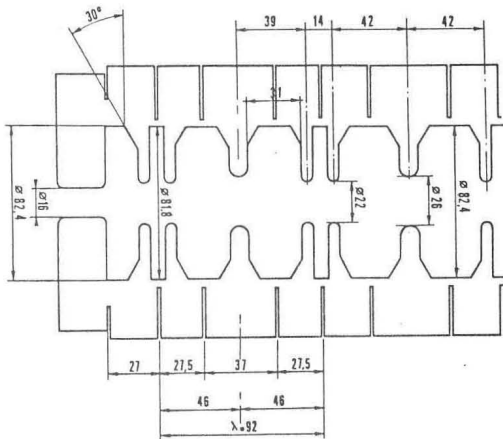


Fig. 4. Sketch of the buncher RF structure.

The 2 first wavelengths are shortened to 9.2 and 9.8 cm in order to fit the electron input speed. The RF feedthrough is located at the end of the structure. So, the cylindrical symmetry of the input RF fields is perfect and there is no discontinuity in the focusing magnetic field.

The calculated shunt impedance (from Super Fish) is $38 \text{ M}\Omega/\text{m}$ leading to a unloaded energy of 30.3 MeV at the nominal power of 11 MW, and a beam loading figure of : 0.0563 MeV/nC.

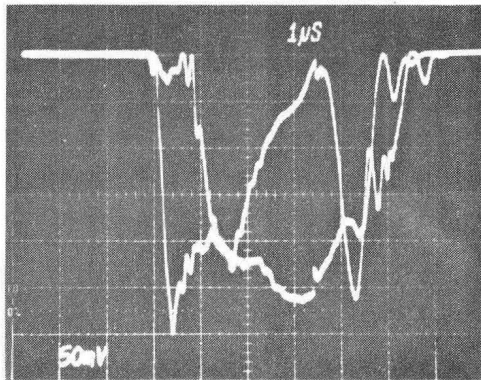


Fig. 5. Buncher RF pulse : internal and reflected wave form.

A prebuncher pill-box cavity is located 7.5 cm ahead of the internal part of the buncher cut-off tube.

The beam path from the gun anode to the end of the buncher is completely immersed in a 0.2 T magnetic field.

1.2 . Beam lines

The straight beam line is designed to measure the beam emittance by the "3 length" method.

It is so equipped with 3 profile monitors located 3 meters apart of each other ; a profile monitor is a 4 nut collimator which may be used as a horizontal or vertical movable slot, associated with a intensity monitor.

An horizontal magnetic spectrometer associated with an ajustable slot and an intensity monitor allows beam energy and energy spread measurement to a resolution of 0.5 %.

The RF phase spread of the microbunch may also be measured by means of a RF T.W. 20 cm deflecting structure fed through a sensitive high power phase shifter and associated with the second collimator.

The maximum deflection sensitivity is : 1 mR/d° at 25 MeV for our available input power of 3.6 MW. The vertical RF deflection associated with the horizontal spectrometer allows a simultaneous analysis in phase and energy.

Intensity monitors give the peak current and pulse shape ; associated with a fast integrator they also give the electrical beam charge over the whole pulse.

2 - Experimental results

2.1 . Accelerated intensity and charge

The capture efficiency is found to be very good. We measured at the end of the buncher through a square hole of $7 \cdot 7 \text{ mm}^2$ up to :

- peak intensity : 15 A ($3 \cdot 10^{10} \text{ e}^-/\text{microbunch}$)
- electrical charge per pulse : 300 nanoC.

Without specific attempt to get higher figures as these ones are far above the nominal values of the LIL project.

The other beam parameters were measured at 3 typical charge values at the buncher output :

- negligible beam loading 3 nanoC.
- 50 nanoC.
- 100 nanoC.

2.2 . Energy - Energy spread

Energy spectra have been systematically measured for several accelerated charges. Three typical ones corresponding to the nominal RF power of 11 MW and accelerated charges of 3, 50 and 100 nanoC are given on fig. 6. Prebuncher parameters have been ajusted for optimisation. The unloaded energy is found to be 29.5 MeV and the energy spreads containing 80 % of the electrons to be 5, 11.5 and 19.6 %.

The beam loading effect also appears as an electric field drop. The corresponding RF signal is picked up by an internal loop, rectified and displayed on an oscilloscope.

We appreciated so a field drop of 11 % for an accelerated charge of 50 nanoC. This figure is compatible with the expected one.

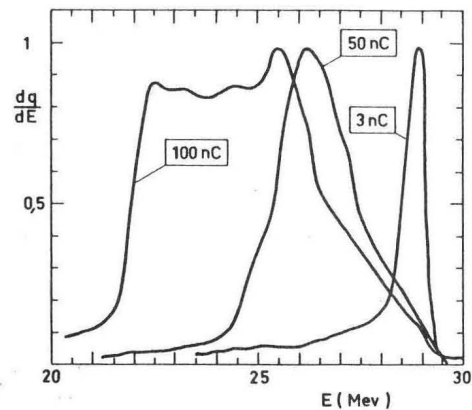


Fig. 6. Typical energy spectra for 3, 50 and 100 nC.

2.3 . Emittance (Ref. 2)

Beam profiles are measured at 3 successive distances from the buncher output : .5, 3.5, 6.5 m right after the collimators 1, 2 and 3. Typical graphs are shown on fig. 7. Each profile is fitted by a gaussian curve of same surface, the standard deviation of which σx_i is taken as the characteristic parameter.

From $\sigma x_1, \sigma x_2, \sigma x_3$ are calculated the standard transverse deviation σx at the cross over, the standard angular deviation $\sigma \theta$, and the emittance surface S containing 80 % of the particules in each direction horizontal (H) and vertical (V) for an accelerated charge per pulse, q , of 50 an 100 nanoC.

q		σx_1	σx_2	σx_3	σx	$\sigma \theta$	$\frac{1}{\pi} S$	$\Delta S/S$
50	H	2.14	5.42	10.80	2.06	1.86	12.36	$\pm 11 \%$
	V	1.76	5.87	12.46	1.45	2.23	10.40	$\pm 17 \%$
100	H	1.84	6.06	12.06	1.81	2.05	11.90	$\pm 18 \%$
	V	1.56	6.50	13.03	1.53	2.21	10.87	$\pm 7 \%$

σx is given in mm, $\sigma \theta$ in mR, q in nC.
 $\Delta S/S$ is the relative error on S assuming a experimental error ≤ 0.2 mm on the σx_i .

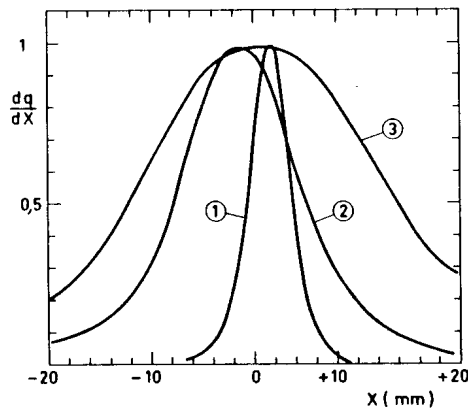


Fig. 7. Beam profiles at collimators 1, 2 and 3.

2.4 . Phase spread of the microbunch

What is measured is a global value including the phase spread of the individual microbunches and the phase shift from the first to the last microbunch.

This value is actually the interesting one because it will make the total energy spread of the positron beam.

From the graphs (see a typical one at 50 nC on fig. 8) one has calculated the charge distribution i.e. the charge percentage $\Delta q/q$ within an RF phase spread $\Delta \phi$:

$\Delta \phi$ (d°)		2.5	5	10	15	20	30	45	55
(50 nC)	$\Delta q/q$ (%)	14	27	44	54	61	70	80	86
(100 nC)		10	20	36	46	53	62	74	80

These results are pessimistic :

. The resolution of the measurement is estimated to be : 2.4 d° (Ref. 3). So the width of the bunch peak is found larger than the actual one.

. The transverse dimension of the bunch tail is larger than the peak one. So the contribution of the tail is overestimated.

The microbunch is also found to be tilted along the longitudinal axis. So we were able to cut off the tail without losing too much on the peak by narrowing the upstream collimator Nb. 1.

It is noticeable that the narrowest phase spreads do not correspond to the best energy spectra.

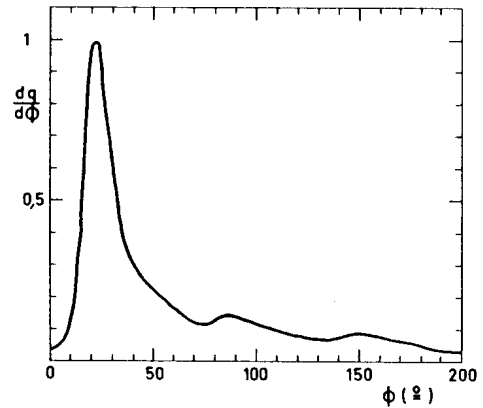


Fig. 8. Microbunch phase spread at 50 nC.

References

1. D. Tronc.
Calculs détaillés de la tête expérimentale d'accélérateur à électrons pour le LEP.
C.G.R. MeV, ST 8029, May 80.
2. R. Belbeoch
Mesure de l'émittance transverse d'un faisceau d'électrons à la sortie du groupeur LEP.
LAL/PI 84-11/T, February 21, 1984.
3. R. Belbeoch.
Pouvoir de résolution dans la mesure de longueurs des paquets à la sortie du groupeur de LEP.
LAL/PI to be published.